JCB Report

Transferrin receptor recycling in the absence of perinuclear recycling endosomes

David Sheff, Laurence Pelletier, Christopher B. O'Connell, Graham Warren, and Ira Mellman

Department of Cell Biology, Ludwig Institute for Cancer Research, Yale University School of Medicine, New Haven, CT 06520

In mammalian cells, internalized receptors such as transferrin (Tfn) receptor are presumed to pass sequentially through early endosomes (EEs) and perinuclear recycling endosomes (REs) before returning to the plasma membrane. Whether passage through RE is obligatory, however, remains unclear. Kinetic analysis of endocytosis in CHO cells suggested that the majority of internalized Tfn bypassed REs returning to the surface from EEs. To determine directly if REs are dispensable for recycling, we studied Tfn recycling in cytoplasts microsurgically created to contain peripheral EEs but to exclude perinuclear REs. The cytoplasts actively internalized and recycled Tfn. Surprisingly, they also exhibited spatially and temporally distinct endosome populations. The first appeared to correspond to EEs, labeling initially with Tfn, being positive for early endosomal antigen 1 (EEA-1) and containing only small amounts of Rab11, an RE marker. The second was EEA-1 negative and with time recruited Rab11, suggesting that cytoplasts assembled functional REs. These results suggest that although perinuclear REs are not essential components of the Tfn recycling pathway, they are dynamic structures which preexist in the peripheral cytoplasm or can be regenerated from EE- and cytosol-derived components such as Rab11.

Introduction

Mammalian cells continuously internalize their plasma membrane proteins and lipids during the ongoing process of clathrin-mediated endocytosis (Mellman, 1996). Receptor–ligand complexes are first delivered to early endosomes (EEs)* in which the acidic pH is sufficient to facilitate the dissociation of many ligands from their receptors. Discharged ligands are sorted to late endosomes and lysosomes for degradation. The receptors, along with many other internalized plasma membrane proteins and lipids, escape degradation by accessing one or more recycling pathways returning to the plasma membrane. Recycling is thought to be mediated by vesicular carriers that transfer receptors to a tubulovesicular compartment referred to as recycling endosomes (REs) (Yamashiro et al., 1984; Trowbridge et al., 1993). In CHO and other cell types, REs are perinuclear and tightly associated with the microtubule organizing center. Biochemically, REs are enriched in the GTPase Rab11 and the v-SNARE vesicle-associated membrane protein 3 (VAMP-3) (Daro et al., 1996; Ullrich et al., 1996; Bajno et al., 2000). REs may also serve as a storage depot for plasma membrane components (Bajno et al., 2000; Pierini et al., 2000). In contrast to REs, EEs are enriched in Rab4, Rab5, and early endosomal antigen 1 (EEA-1) although they also contain at least some VAMP-3 and Rab11 (Sönnichsen et al., 2000).

Much of what we know concerning the traffic through EEs and REs has emerged from study of the transferrin (Tfn) and Tfn receptor (TfnR) in CHO cells. Unlike many other ligands, Tfn remains bound to its receptor throughout the recycling pathway and is released upon returning to the cell surface (Mellman, 1996). Recycling Tfn may not simply pass sequentially through EEs and REs, as recycling is typically biphasic with both initial rapid and later slow components (Daro et al., 1996). At least in polarized MDCK cells, the two rates may reflect a rapid passage of the majority (65%) of Tfn directly back from EEs to the plasma membrane or a slower route that requires additional passage through REs (Sheff et al., 1999). Furthermore, expression of dominant negative Rab11 (in polarized epithelial cells) specifically inhibits the slow (RE) phase of Tfn recycling (Ullrich et al., 1996). Lipid and Tfn recycling were initially thought to exhibit identical kinetics (Mayor et al., 1993), but more recent work has suggested that only lipids (i.e., lipid analogs) participate in a rapid (e.g., EE only) recycling pathway (Hao

The online version of this article contains supplemental material.

Address correspondence to Ira Mellman, Department of Cell Biology, Ludwig Institute for Cancer Research, Yale University School of Medicine, 333 Cedar Street, P.O. Box 208002, New Haven, CT 06520. Tel.: (203) 785-4303. Fax: (203) 785-4301. E-mail: ira.mellman@yale.edu

David Sheff and Laurence Pelletier contributed equally to this work.

*Abbreviations used in this paper: EE, early endosome; EEA-1, early endosomal antigen 1; RE, recycling endosome; Tfn, transferrin; VAMP-3, vesicle-associated membrane protein 3.

Key words: endocytosis; recycling; transferrin; biogenesis; cytoplast

© The Rockefeller University Press, 0021-9525/2002/3/797/8 $5.00

Downloaded from http://rupress.org/jcb/article-pdf/156/5/797/1302370/jcb1565797.pdf by guest on 25 September 2022

and Maxfield, 2000). At present, there are few quantitative data on the relative fractions of Tfn that recycle directly from EEs versus traversing through REs. It is even possible that passage through the RE is obligatory for recycling.

The relationship between EEs and REs remains unclear despite the fact that they are kinetically distinct, often (but not always) having distinct distributions in the cell, and are associated with different Rabs (Daro et al., 1996; Ullrich et al., 1996; Trischler et al., 1999). REs may be autonomous organelles which, like the Golgi apparatus, cannot be reformed from upstream organelles despite being connected by continuous membrane traffic (Klumperman, 2000; Pelletier et al., 2000). Alternatively, REs may be largely derived from components also found in EEs in a fashion similar to the maturation of EE to late endosomes (Mellman, 1996). Consistent with the latter possibility, both Rab4 and Rab11 can be observed on separate domains of the same EE (Sönnichsen et al., 2000). In this case, vesicular traffic from EEs, perhaps in combination with recruitment of cytosolic factors, should be capable of reconstituting functional REs.

Here we use both kinetic analysis in intact cells and fluorescence imaging of microsurgically created cytoplasts (Pelletier et al., 2000) to show that Tfn recycling can bypass perinuclear REs, although the peripheral cytoplasm nevertheless has the capacity to assemble RE-like structures autonomously.

Results and discussion

Tfn passes through both peripheral EEs and perinuclear REs during the course of recycling to the plasma membrane in CHO cells transfected with human TfnR (CHO-hTfnR) (Yamashiro et al., 1984; Daro et al., 1996; Mellman, 1996). We sought to determine what fraction of recycling traffic actually passed through REs by adapting a kinetic analysis of Tfn recycling developed for polarized MDCK cells (Fig. 1 A) (Sheff et al., 1999). We used a model with two intracellular compartments (EEs and REs) from both of which Tfn recycling might occur (Fig. 1 A). Inclusion or omission of other compartments did not provide a statistically better fit to our experimental data.

Recycling of Tfn was assessed by monitoring ^{125}I-Tfn release into the medium (Fig. 1 B) (Sheff et al., 1999). The rate of surface clearance (k_1) was 0.311 min^{-1} (Fig. 1 A and Video 1), similar to that observed for basolaterally bound Tfn in MDCK cells (Sheff et al., 1999).

We applied a model comprised of first order rate equations (supplemental text) to derive rate constants from the experimental data. Fit of the model to each data set were optimized by minimizing the sum-squared error (SSE) (Motulsky and Ransnas, 1987). The best fit for the summed data sets ($n = 9$) yielded an SSE = 333. Derived rate constants are shown in Fig. 1 A. Supplemental materials are available at http://www.jcb.org/cgi/content/full/jcb.200111048/DC1.

Fischer's F test was used to assess whether one model fit the combined data sets significantly better than did another. The two compartment model fit better than alternatives requiring passage through the RE ($F = 201$, $P < 0.005$) or having a single endocytic compartment ($F = 16$, $P < 0.005$) (Daniel, 1987). Extrapolation of the kinetics of appearance of Tfn in the two compartments, suggested peak amounts in the EEs and REs occurring within 3 and 20 min, respectively (Fig. 1 B). However, EEs were maximally resolvable from REs at 2 min as were REs from EEs at 25 min (Fig. 1 B, arrow). We therefore defined EEs as those endosomes accessible to Tfn after 2 min of internalization and REs as structures labeled after 25 min (Fig. 1 B, arrows).

Using the derived values, 76% of recycled Tfn proceeded solely through EEs while 24% also traversed through REs. This result is consistent with our earlier finding that 65% of Tfn traffic bypasses the RE in polarized MDCK cells. This suggests that the ability to bypass REs is not solely restricted to polarized cells as had been suggested (Hao and Maxfield, 2000). Thus, at a minimum, passage through the RE is not obligatory.

Hao and Maxfield reported that lipid traffic from EE to plasma membrane (0.45–0.53 min^{-1}) is faster than we report for Tfn traffic (0.15 min^{-1}). This difference is surprising in light of colocalization of lipophilic dyes with Tfn in EEs and the overall similar recycling kinetics between Tfn and lipids observed previously in CHO cells (Mayor et al., 1993; Mukherjee et al., 1999). However, variations in methods used to monitor recycling (biochemical vs. microscopic assays) might explain this discrepancy.

Because the bulk of internalized Tfn was predicted to recycle without reaching REs, we devised an assay to determine directly if passage through perinuclear REs is obligatory for recycling. We used microsurgery to separate peripheral portions (cytoplasts) from the bulk of CHO-hTfnR cells containing the nucleus (karyoplasts) (Maniotis and Schliwa, 1991; Pelletier et al., 2000). REs were selectively labeled with a Alexa 594–Tfn internalized for 25 min, under which conditions Tfn was restricted to the perinuclear region. Cytoplasts were then generated using microneedles drawn across peripheral cellular projections (Fig. 1 C and Video 1). Visible perinuclear REs were excluded from the resulting cytoplasts as judged by the lack of Tfn-positive structures. However, peripheral Tfn-labeled structures below our limit of detection may have remained in the cytoplast. Videos are available at http://www.jcb.org/cgi/content/full/jcb.200111048/DC1.

After allowing for a 30–60 min recovery period, Alexa 594-Tfn was bound to the surface of both cytoplasts and karyoplasts. Upon warming to 37°C for 2 min, Tfn entered small punctate structures in the periphery of both the cytoplasts (c) and karyoplasts (k) (Fig. 1 D, 2 min). After 7 min, Tfn was observed in both peripheral EEs and perinuclear REs in the karyoplasts, although fewer total individual fluorescent structures were visible. Much the same was also true for the cytoplasts, although there was no spatial redistribution (Fig. 1 D, 7 min). After 25 min, perinuclear REs were the predominant labeled structures in the karyoplasts (Fig. 2 D, 25 min). Cytoplasts were still labeled although fewer structures were observed. After 45 min, all detectable Tfn had disappeared from both karyoplasts and cytoplasts (Fig. 2 D, 45 min). At no time did Alexa 594–Tfn enter lysosomes in cytoplasts or karyoplasts as judged by colocalization with fluid phase markers (unpublished data). Thus, the time course of recycling in cytoplasts was similar to that in uncut cells, suggesting that traffic through perinuclear REs was not

Downloaded from http://rupress.org/jcb/article-pdf/156/5/797/1302370/jcb1565797.pdf by guest on 25 September 2022

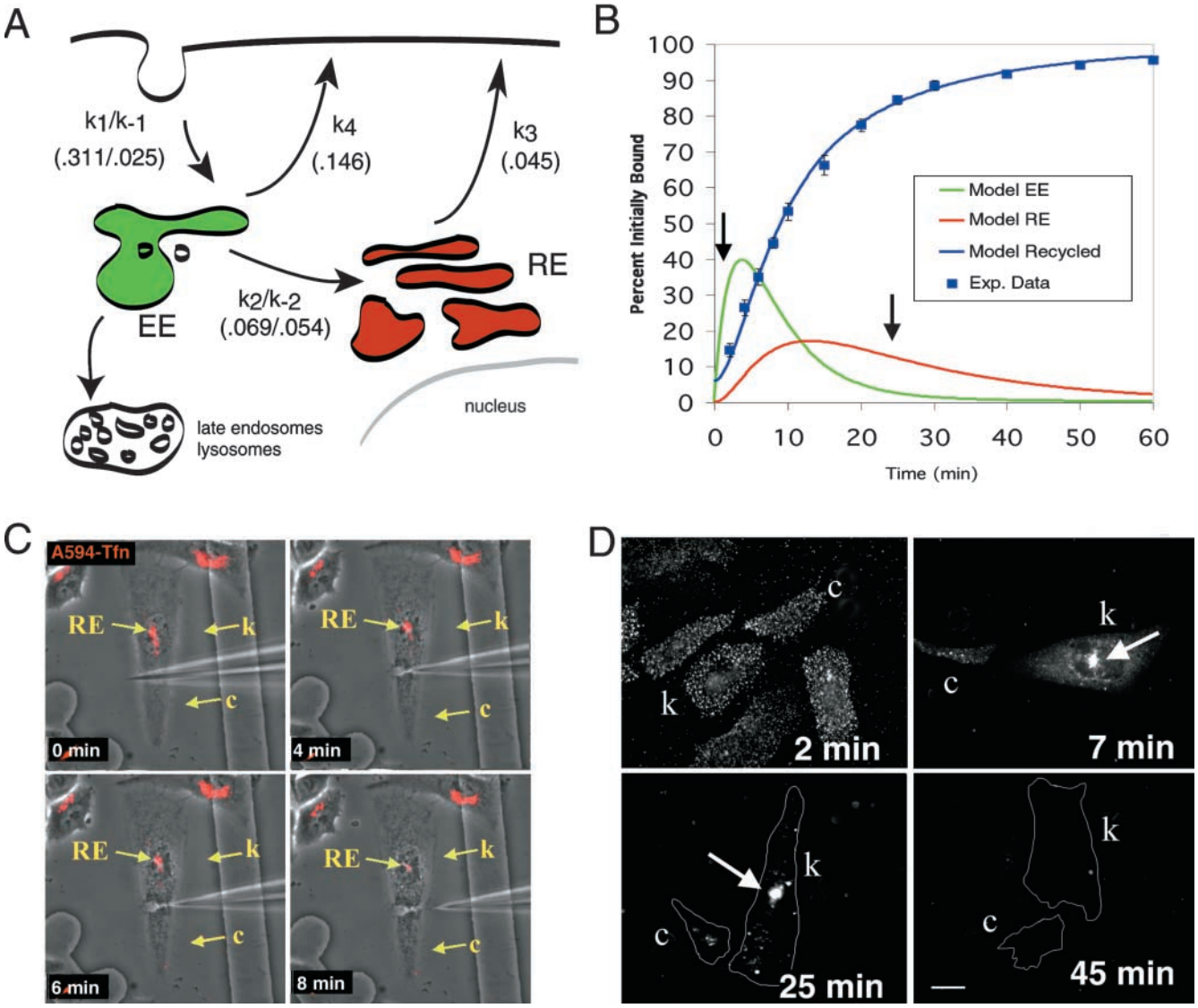

Figure 1. **Tfn recycling in CHO-TfnR cell and cytoplasts.** (A) Diagram of rate constants and pathways derived from the mathematical model used to interpret recycling data. (B) Fit of model to experimental data. Predicted recycling curves (blue line) were fit to recycling data (blue squares). The expected percentage of Tfn to be in EE (green line) and RE (red line) over time are shown. Note the relative distribution of Tfn at 2 and 25 min (arrows). Values for each data point were averaged and shown as the mean ± SD ($n = 9$). (C) CHO-TfnR cells bound with Alexa 594–Tfn on ice were chased 25 min at 37°C to label REs (red channel). Overlaid phase and fluorescence images 0, 4, 6, and 8 min into microsurgery are shown and the resulting karyoplast (k) and cytoplast (c) indicated. Panels were extracted from Video 1. (D) After microsurgery, Alexa 594–Tfn was bound to the cell surface on ice, internalized at 37°C for the indicated times before fixation. Cytoplasts (c) and the karyoplasts (k) are shown. Arrows point to the REs in karyoplasts (7 and 25 min). Cells were outlined for clarity. Video 1 is available at http://www.jcb.org/cgi/content/full/jcb.200111048/DC1. Bar, 10 μm.

obligatory for complete Tfn recycling. Recycling proceeded to completion, suggesting that either all recycling in cytoplasts was at the level of EEs or that the functional equivalent of perinuclear REs were present in the cytoplasts. This result is in sharp contrast to that obtained using cytoplasts to study the secretory pathway. Cytoplasts devoid of Golgi elements but containing ER were unable to deliver newly synthesized membrane proteins from the ER to the cell surface even after lengthy incubations (Pelletier et al., 2000).

To determine if cytoplasts contained only EEs or kinetically distinct endosome populations, we used a dual labeling approach in which Alexa 594–Tfn was internalized for 25 min and Alexa 488–Tfn then internalized for 2 min. In both uncut cells and karyoplasts, the longer pulse of Tfn (red) as expected labeled perinuclear REs (Fig. 2, A and C). The brief Tfn pulse (green), also as expected, labeled peripheral EEs (Fig. 2, B and C). Unexpectedly, however, a similar situation was observed in cytoplasts. As seen in the insets to Fig. 2, the brief (green) Tfn pulse yielded a pattern of small endosomes spread throughout the cytoplasm, but the longer (red) pulse labeled a distinct population, fewer in number (Fig. 2, arrows). The latter differed from REs in the uncut cells by being more dispersed. Thus, cytoplasts contain two kinetically distinct populations of endosomes, the first corresponding to EEs and the second to some type of transport intermediate or to REs unexpectedly present or reassembled in the peripheral cytoplasm.

Downloaded from http://rupress.org/jcb/article-pdf/156/5/797/1302370/jcb1565797.pdf by guest on 25 September 2022

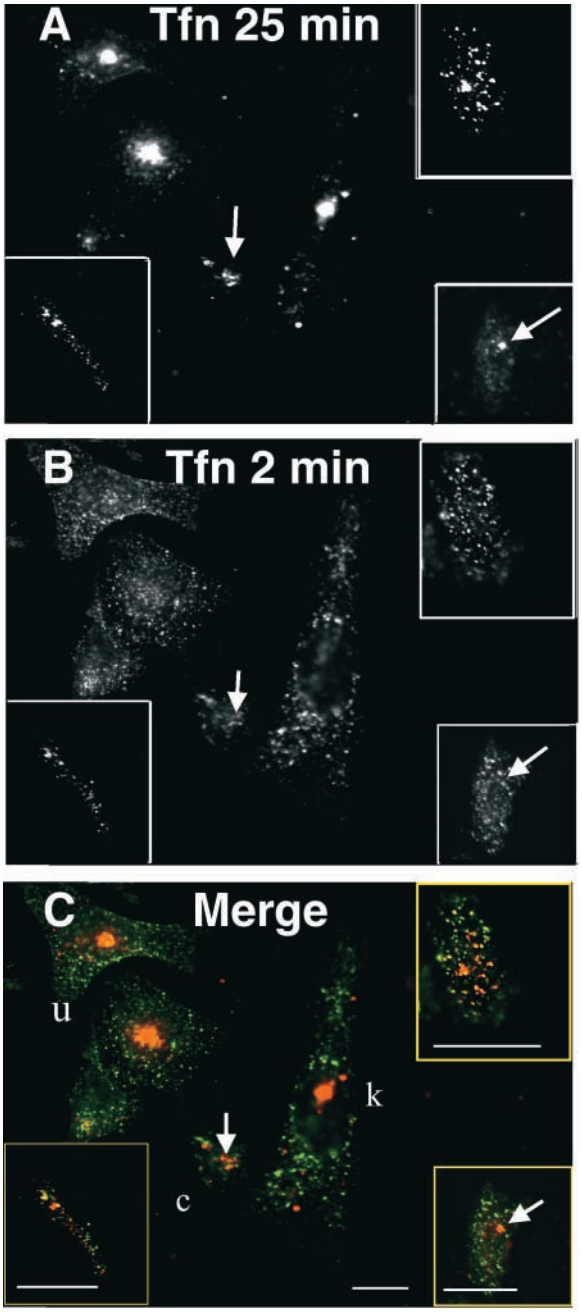

Figure 2. **Tfn passes through two spatially and temporally distinct endocytic compartments in cytoplasts.** Alexa 594–Tfn was bound to the surface of normal and cut cells (on ice) and internalized for 25 min (A, to label REs) before being subjected to a final 2 min pulse of Alexa 488–Tfn (B, to label EEs). The cells were fixed in PFA, mounted, and analyzed by fluorescence microscopy. Typical labeling patterns of uncut cells are shown (u). A cytoplast and accompanying karyoplast (c and k) are shown for comparison. Cytoplasts from three independent experiments are shown in insets. Arrows indicate the compartment labeled at a longer time in cytoplasts. (C) Merged image of Alexa 594–Tfn (red, 25 min) and Alexa 488–Tfn (green, 2 min). Bars, 10 μm.

To test whether endosomes in cytoplasts corresponded biochemically to EEs and REs, we labeled the cytoplasts with established markers for these two populations of endosomes. EEs were labeled with antibodies to the EE-specific marker EEA-1 (Mu et al., 1995; Waite et al., 1998; Christoforidis et al., 1999). To label REs, CHO-hTfnR cells were transfected with a cDNA encoding Rab11-GFP, shown previously to colocalize with endogenous Rab11 primarily in REs (Ullrich et al., 1996; Sönnichsen et al., 2000).

A significant fraction of Tfn internalized for 2 min was found in endosomes that also labeled for EEA-1 in uncut cells, karyoplasts, and cytoplasts (Fig. 3 A). As often described previously, colocalization was incomplete (see insets and arrows) (Mu et al., 1995). The Tfn-containing structures were clearly distinct, however, from the bulk of the RE population as most of the Rab11-positive structures were negative for Tfn in uncut cells (unpublished data), cytoplasts, and karyoplasts (Fig. 3 B).

After 25 min, Tfn internalized by both karyoplasts and cytoplasts no longer colocalized with EEA-1 (Fig. 3 C), but was found in structures strongly positive for Rab11-GFP (Fig. 3 D). In karyoplasts, as in uncut cells (unpublished data), structures positive for both Tfn and Rab11-GFP were found predominantly in the perinuclear cytoplasm. In cytoplasts, Tfn again colocalized with brightly Rab11-GFP–labeled structures although these were distributed throughout the cytoplasm (Fig. 3 D, arrows). Note that all of the cytoplast images showing Rab11-GFP in Fig. 3 were digitally enhanced to optimize the fluorescence signal. In typical cells, the maximum pixel intensity in the perinuclear region was >20 times brighter than found in labeled peripheral structures. The cytoplasts were found to contain only 10–15% of the total cell Rab11-GFP signal present before microsurgery. Although this percentage did not change following microsurgery, Rab11-GFP in the cytoplasts did exhibit a spatial redistribution as a function of time (see below).

To further characterize the identity of the second endosomal population in cytoplasts, we monitored sensitivity of to AlF_4^-. Treatment of intact cells with this agent resulted in retention of Tfn in REs in MDCK cells (Sheff et al., 1999), and our kinetic analysis here suggested that the retention resulted from inhibition of traffic along the RE exit pathway even in CHO cells (unpublished data). Internalized Tfn in AlF_4^--treated CHO cells, karyoplasts, and cytoplasts was localized in a subset of EEA-1–negative, Rab11-GFP–positive endosomes, presumably REs (Fig. 3, E and F, arrows). Interestingly, the Tfn was not lost from karyoplasts or cytoplasts even after 50 min of chase, at which time Tfn would have been completely recycled from untreated cells or cytoplasts (compare Fig. 3 E to Fig. 1 D).

Thus, cytoplasts contained two distinct populations of endosomes. The first was labeled both by Tfn internalized for 2 min and by antibodies to EEA-1; accordingly, they can be considered EEs. The second was labeled by Tfn internalized for 25 min, EEA-1 negative, and more strongly labeled by Rab11-GFP. In addition, exit from the second population was inhibited by AlF_4^-. By these criteria, the second population was functionally and biochemically defined as REs.

Since these Rab11-positive REs were absent from the peripheral regions of cells before microsurgery, where did they come from? One possibility is that in intact cells, a fraction of REs are normally found in the periphery, spatially distinct from the major RE population in the perinuclear region. Such peripheral RE "seeds" may be below our limit of detection, but if present, their reorganization could explain the apparent reappearance of RE in cytoplasts.

Downloaded from http://rupress.org/jcb/article-pdf/156/5/797/1302370/jcb1565797.pdf by guest on 25 September 2022

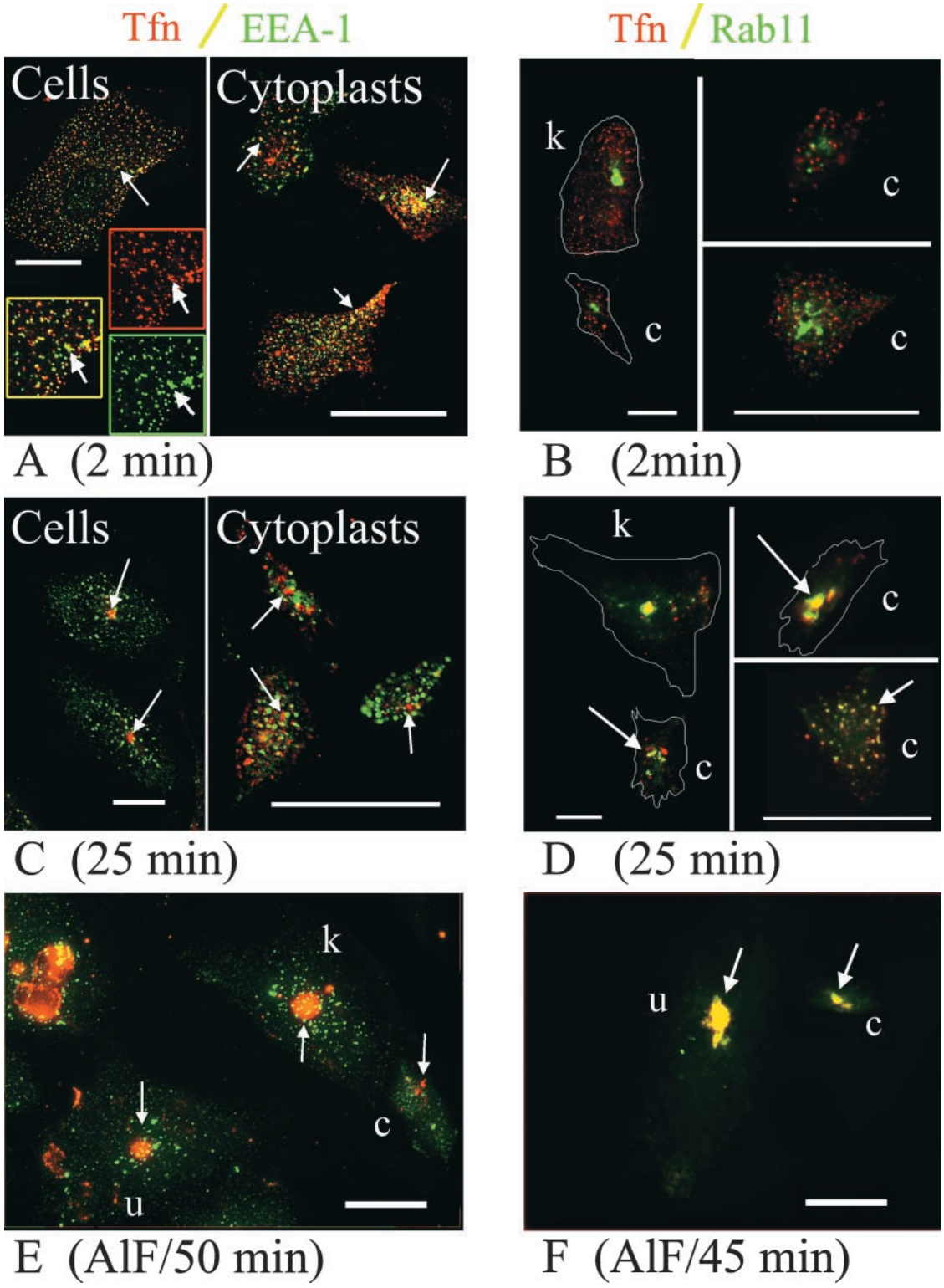

Figure 3. **Cytoplasts contain bona fide EE and RE.** CHO-TfnR cells were submitted to microsurgery to create karyoplasts (k) and cytoplasts (c). Both are outlined in some cases for clarity. (A) Cytoplasts and cells internalized Alexa 594–Tfn (red) for 2 min before fixation, then labeled for EEA-1 (green). Arrows indicate colocalization of Tfn and EEA-1 (yellow). Insets in A are a magnification of the uncut cell periphery. (B) Cytoplasts generated from Rab11-GFP–expressing cells were allowed to internalize Alexa 594–Tfn (red) for 2 min before fixation. (C and D) Cells prepared as in A and B but Alexa 594-Tfn internalized for 25 min (E and F). Cells prepared as in A and B but treated with AlF_4^- during the chase period and Tfn internalized for the indicated times. Arrows indicate Tfn (red) containing endosomes. Bars, 10 μm.

An alternative possibility is that Rab11-positive REs in the cytoplasts were formed largely de novo from components already distributed throughout the recycling pathway and the cytosol. RE membrane proteins such as VAMP-3, found in REs, EEs, and the plasma membrane at equilibrium (Daro et al., 1996; Sönnichsen et al., 2000), might give rise to REs as

Downloaded from http://rupress.org/jcb/article-pdf/156/5/797/1302370/jcb1565797.pdf by guest on 25 September 2022

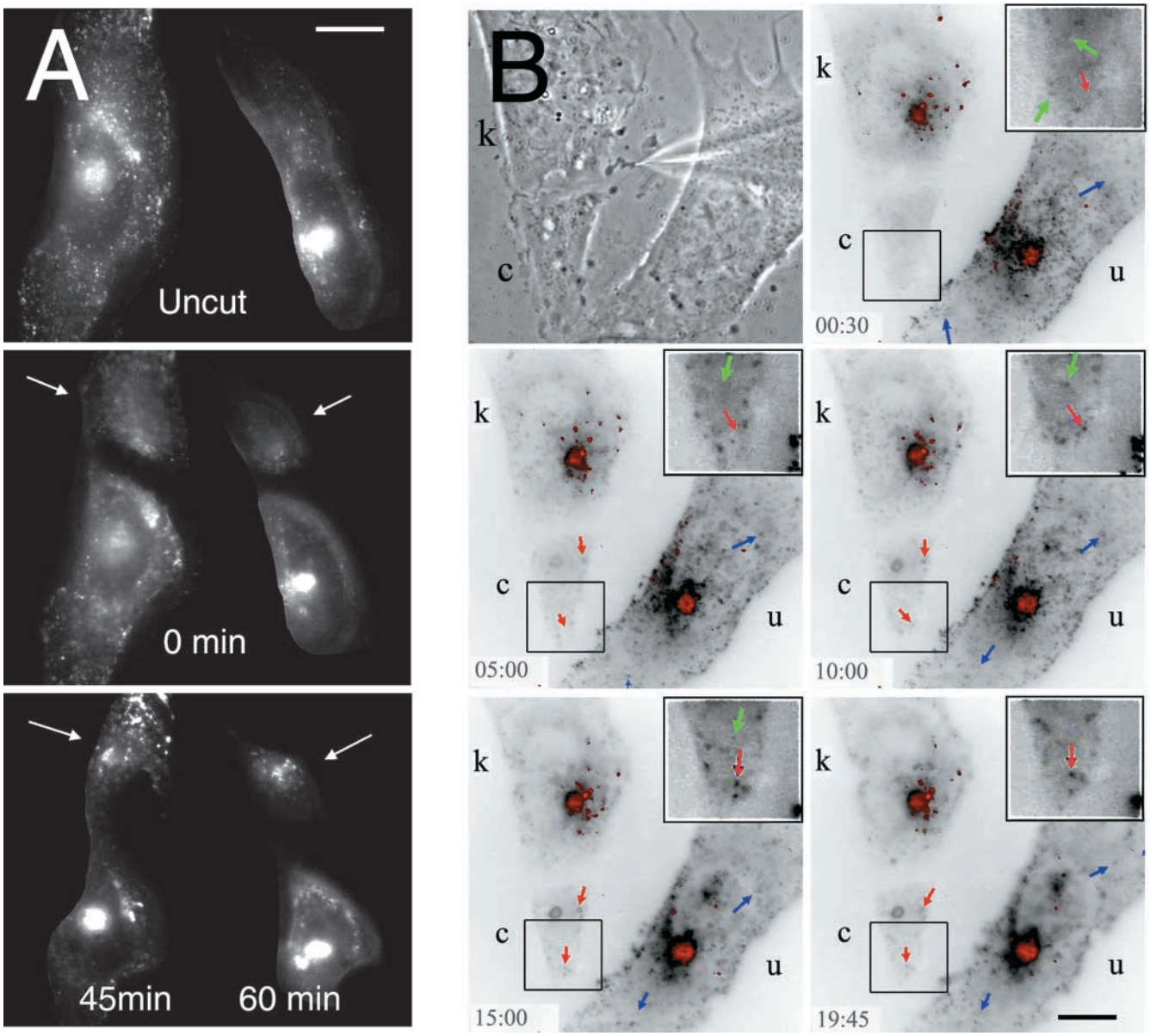

Figure 4. **Rab11-GFP recruitment in cytoplasts.** (A) CHO-TfnR cells expressing Rab11-GFP were submitted to microsurgery. Fluorescence images were acquired either before (Uncut), immediately after (0 min), or 45–60 min after microsurgery to assess the formation of Rab11-positive structures in the cytoplasts. Arrows indicate cytoplasts. The two cells shown are from separate experiments. (B) CHO-TfnR cells expressing Rab11-GFP were submitted to microsurgery before time-lapse video microscopy. Exposures were adjusted to visualize peripheral Rab11 structures, while overexposing perinuclear regions. One phase contrast image of a cut cell is shown. Panels are inverted images of the GFP (black on white) overlain with synchronous contrast enhanced Tfn images (red) at 0:30, 5:00, 10:00, 15:00, and 19:45 (min:s). Cytoplast (c), karyoplast (k), and uncut cell (u) are shown. Insets are a magnified, contrast-enhanced view of the boxed region of the cytoplast. Red arrows indicate RE-like structures that recruit Rab11-GFP throughout the time-course. Green arrows indicate structures in the cytoplast that initially recruit Rab11-GFP but fade to the limit of detection over time. In contrast, Rab11-GFP–positive EE remain stable in position and intensity over time in uncut cells (blue arrows). Images in B were extracted from Video 2. Video 2 is available at http://www.jcb.org/cgi/content/full/jcb.200111048/DC1. Bars, 10 μm.

a consequence of normal recycling activity much as late endosomes are thought to form by maturation from EEs on the lysosomal pathway (Schmid et al., 1988; Mellman, 1996).

Sönnichsen et al. (2000) have shown that Rab11 is present in limited quantities on EEs. The EE membrane is laterally differentiated into distinct subdomains marked by different endosome-associated Rab proteins (Rabs 4, 5, and 11). We also observe this phenomenon using longer exposures in our CHO-hTfnR cells expressing Rab11-GFP. Rab11-positive structures in the periphery that colocalized with Tfn internalized for 2 min, characteristic of EEs (Fig. 4, A and B, and unpublished data). These domains, defined by the presence of Rab11, might give rise to vesicles or tubules that progressively regenerate a RE population.

We next characterized the appearance of Rab11-positive REs in the peripheral cytoplasm. Rather than "resting" microsurgically altered cells for ~30 min before imaging (as in all experiments described thus far), we examined the kinetics of

Downloaded from http://rupress.org/jcb/article-pdf/156/5/797/1302370/jcb1565797.pdf by guest on 25 September 2022

Rab11-GFP redistribution immediately after microsurgery. If REs in cytoplasts arose from expansion of preexisting "seed" organelles, then Rab11-GFP might be directly recruited from the cytoplasm to these organelles or possibly coalesce to become more visible. Alternatively, if REs were assembled from EE traffic either de novo or by targeting of this traffic to RE "seed" organelles, then Rab11-GFP would first be visualized on EE domains throughout the cytoplast and then move to a steady-state distribution as the REs are reestablished.

CHO-hTfnR cells transfected with Rab11-GFP were pulsed with Alexa 594–Tfn to preferentially label perinuclear REs as above. Peripheral regions of cells used for microsurgery contained little in the way of intense Rab11 signal either before (Fig. 4 A, top) or immediately after (Fig. 4 A, middle) microsurgery. 10–15% of the total GFP fluorescence was included in the cytoplast (12–18% of the cell volume) either in the cytosol or associated with membranes beneath the level of detection. Within 45–60 min, however, the cytoplasts developed Rab11-GFP–positive structures that were substantially brighter, even more so than the structures seen in the periphery of their respective karyoplasts (Fig. 4 A, bottom).

These events were next visualized by time-lapse video microscopy (Fig. 4 B and Video 2). Tfn-labeled REs (red; labeled by a 25 min Tfn pulse before filming) were imaged simultaneously with Rab11-GFP (black) in the cytoplast (c), karyoplast (k), and uncut cells (u). Exposures were adjusted to optimize detection of peripheral Rab11 structures, thus overexposing perinuclear regions. Immediately after microsurgery, the cytoplasts contained no discernible Tfn, suggesting that perinuclear REs were successfully excluded. Only weak Rab11-GFP staining was associated with vesicular structures. Within 5 min, the intensity of Rab11-GFP labeling of individual structures began to increase (Fig. 4 B and Video 2; red arrows). Some structures that were weakly positive became more intensely labeled during the next 60 min (red arrows in Fig. 4, enhanced contrast inserts, and Video 2), whereas others seemed to lose Rab11 labeling (green arrows). Fusion or coalescence of labeled structures was not observed in the cytoplasts. Fusion was also not observed in uncut cells, nor was movement of Rab11-positive structures from the periphery to the perinuclear region (Fig. 4 B and Video 2 blue arrows in uncut [u] cell). Videos are available at http://www.jcb.org/cgi/content/full/jcb.200111048/DC1.

Although these results do not provide a definitive test, they do show that even if peripheral REs preexisted in cytoplasts at the time of microsurgery, they become more strongly labeled for Rab11-GFP as a function of time. Since individual fusion events were not observed, the increased labeling may reflect recruitment of Rab11-GFP from a soluble pool. It is important to note, however, that Alexa 594–Tfn was not detected in this presumptive peripheral RE population following labeling of uncut cells for 25 min. They were readily accessed by the fluorescent Tfn, however, when the cytoplasts were allowed to take up the probe after microsurgery. Thus, these results are perhaps more consistent with the possibility that at least some of the Rab11-positive REs found in the cytoplasts were formed by budding events emanating from EEs. In this case, the Rab11-GFP might be recruited first to EEs, which then form Rab11-enriched domains which could dissociate from EEs and thus initiate RE formation essentially de novo (Sönnichsen et al., 2000). Considerably more information will be required, however, before concluding that cytoplasts or intact cells for that matter form REs by this type of maturation event from EEs.

In either event, our results clearly suggest a fundamental difference between the endocytic and exocytic pathways in this system: cytoplasts cannot produce a functional Golgi complex (Pelletier et al., 2000). Either there are insufficient Golgi elements scattered throughout the peripheral cytoplasm, or the ER, present in abundance in cytoplasts, does not contain sufficient quantities of recycling Golgi components to permit regeneration of the Golgi de novo. In contrast, endosomes would appear to comprise a more dynamic population of organelles forming or expanding as required to accommodate membrane flux through the cell. Despite this plasticity they are nonetheless able to form compartments with distinct biochemical and functional identities. Perhaps such dynamic formation of REs is essential to their function as a depot or transit step for intracellular membrane traffic.

Materials and methods

Reagents

All the chemicals used were of analytical grade or better and purchased from Sigma-Aldrich. Alexa 488– and 594–labeled Tfns and secondary antibodies were from Molecular Probes and used at 10 μg/ml. Anti–EEA-1 was from Transduction Labs and used at 20 μg/ml. ^{125}I was from Amersham Pharmacia Biotech.

Cell lines and constructs

CHO cells stably expressing the human Tfn receptor (CHO-TfnR) were generated and maintained as described (Daro et al., 1996). Rab11-GFP clones were provided by Marino Zerial (EMBL, Heidelberg, Germany) and Jonathan Kaggan (Yale University, CT), and transfected into CHO-TfnR cells using FuGENE 6 (F. Hoffmann-La Roche, Ltd.).

Tfn kinetics

Tfn was labeled with ^{125}I as described (Podbilewicz and Mellman, 1990). CHO-TfnR cells were grown to 90% confluence in 6-well or 35-mm cell culture dishes and serum starved for 30 min at 37°C to deplete them of Tfn. Binding and recycling of Tfn was performed as described for MDCK cells except that binding was to the available surface of the cell grown on impermeant cell culture dishes (Sheff et al., 1999). Data handling, equations, and fitting of mathematical models to this data used a two endosomal compartment model as described previously, except that apical pathways were omitted and basolateral pathways were adjusted to represent traffic to the single nonpolarized surface (Sheff et al., 1999). See supplemental text, available at http://www.jcb.org/cgi/content/full/jcb.200111048/DC1.

Tfn and immunolabeling

CHO-TfnR cells grown either on glass coverslips or 175-μm CELLocate-gridded coverslips (Eppendorf) were depleted of Tfn as above, chilled on ice, and allowed to bind Alexa 594-Tfn (60 μg/ml in PBS) for 45 min on ice. Cells were washed briefly in PBS and placed in DME at 37°C for the indicated times. For dual labeling, after 25 min cells were returned to ice and relabeled as above with the second color Tfn. Cells were fixed with 4% paraformaldehyde pH 7.4 in PBS and permeabilized with 0.5% saponin in PBS + 2% BSA (PBS/BSA) for 1 h.

Generation of cytoplasts

Cytoplasts were generated as described previously (Maniotis and Schliwa, 1991; Pelletier et al., 2000). Microneedles were slowly drawn across cell projections over a 7–15 min period so as to maximize the survival of the cytoplasts.

Microscopy and image analysis

Fixed cells were visualized using a ZEISS Axioplan 2 microscope fitted with an Orca II cooled CCD camera (Hamamatsu Phototonic Systems).

Downloaded from http://rupress.org/jcb/article-pdf/156/5/797/1302370/jcb1565797.pdf by guest on 25 September 2022

Live cell imaging was performed on a ZEISS Axiovert 100M fitted with a monochromator (TILL photonics), and a Hamamatsu Orca 100 cooled CCD camera. Both set-ups were driven by the Openlab 3.0.3 image acquisition software package (Improvision). ZEISS Plan-Apochromat® 63× DIC 1.4 NA, 100× DIC 1.4 NA and 100× Phase III 1.4 NA objectives were used. Video images were taken in phase, GFP, and Texas red channels and at 15 or 30 s intervals (for time-lapse imaging) using selective single-pass filter sets (Chroma Technology).

Online supplemental material

Two sets of time-lapse video images of cytoplasts were compiled into TIFF image stacks and converted to QuickTime 5.0 format (Sorenson 3 codec for Video 1, video codec for Video 2) for online publication. Complete equations are provided as a text file. Supplemental material is available at http://www.jcb.org/cgi/content/full/jcb.200111048/DC1.

We are indebted to James Shorter and Friederike Quittnat for their valuable comments on the manuscript. We are grateful to Marino Zerial and Jonathan Kaggan for providing Rab11-GFP constructs. The entire Mellarren lab's support and the stimulating discussions everyone provided were greatly appreciated.

This work was supported by National Institutes of Health grants to I. Mellman and G. Warren, and by the Ludwig Institute for Cancer Research.

Submitted: 13 November 2001
Revised: 15 January 2002
Accepted: 22 January 2002

References

Bajno, L., X.R. Peng, A.D. Schreiber, H.P. Moore, W.S. Trimble, and S. Grinstein. 2000. Focal exocytosis of VAMP3-containing vesicles at sites of phagosome formation. *J. Cell Biol.* 149:697–706.

Christoforidis, S., H.M. McBride, R.D. Burgoyne, and M. Zerial. 1999. The Rab5 effector EEA1 is a core component of endosome docking. *Nature.* 397:621–625.

Daniel, W.W. 1987. Biostatistics: a foundation for analysis in the health sciences. John Wiley and Sons, New York. 127–187 pp.

Daro, E., P. Van der Sluijs, T. Galli, and I. Mellman. 1996. Rab4 and cellubrevin define different early endosome populations on the pathway of transferrin receptor recycling. *Proc. Natl. Acad. Sci. USA.* 93:9559–9564.

Hao, M., and F.R. Maxfield. 2000. Characterization of rapid membrane internalization and recycling. *J. Biol. Chem.* 275:15279–15286.

Klumperman, J. 2000. The growing Golgi: in search of its independence. *Nat. Cell Biol.* 2:E217–E219.

Maniotis, A., and M. Schliwa. 1991. Microsurgical removal of centrosomes blocks cell reproduction and centriole generation in BSC-1 cells. *Cell.* 67:495–504.

Mayor, S., J.F. Presley, and F.R. Maxfield. 1993. Sorting of membrane components from endosomes and subsequent recycling to the cell surface occurs by a bulk flow process. *J. Cell Biol.* 121:1257–1269.

Mellman, I. 1996. Endocytosis and molecular sorting. *Annu. Rev. Cell Dev. Biol.* 12:575–625.

Motulsky, H.J., and L.A. Ransnas. 1987. Fitting curves to data using nonlinear regression: apractical and nonmathematical review. *FASEB J.* 1:365–374.

Mu, F.T., J.M. Callaghan, O. Steele-Mortimer, H. Stenmark, R.G. Parton, P.L. Campbell, J. McCluskey, J.P. Yeo, E.P. Tock, and B.H. Toh. 1995. EEA1, an early endosome-associated protein. EEA1 is a conserved alpha-helical peripheral membrane protein flanked by cysteine "fingers" and contains a calmodulin-binding IQ motif. *J. Biol. Chem.* 270:13503–13511.

Mukherjee, S., T.T. Soe, and F.R. Maxfield. 1999. Endocytic sorting of lipid analogues differing solely in the chemistry of their hydrophobic tails. *J. Cell Biol.* 144:1271–1284.

Pelletier, L., E. Jokitalo, and G. Warren. 2000. The effect of Golgi depletion on exocytic transport. *Nat. Cell Biol.* 2:840–846.

Pierini, L.M., M.A. Lawson, R.J. Eddy, B. Hendey, and F.R. Maxfield. 2000. Oriented endocytic recycling of $\alpha 5\beta 1$ in motile neutrophilis. *Blood.* 95:2471–2480.

Podbilewicz, B., and I. Mellman. 1990. ATP and cytosol requirements for transferrin recycling in intact and disrupted MDCK cells. *EMBO J.* 9:3477–3487.

Schmid, S.L., R. Fuchs, P. Male, and I. Mellman. 1988. Two distinct subpopulations of endosomes involved in membrane recycling and transport to lysosomes. *Cell.* 52:73–83.

Sheff, D.R., E.A. Daro, M. Hull, and I. Mellman. 1999. The receptor recycling pathway contains two distinct populations of early endosomes with different sorting functions. *J. Cell Biol.* 145:123–139.

Sönnichsen, B., S. De Renzis, E. Nielsen, J. Rietdorf, and M. Zerial. 2000. Distinct membrane domains on endosomes in the recycling pathway visualized by multicolor imaging of rab4, rab5, and rab11. *J. Cell Biol.* 149:901–914.

Trischler, M., W. Stoorvogel, and O. Ullrich. 1999. Biochemical analysis of distinct Rab5- and Rab11-positive endosomes along the transferrin pathway. *J. Cell Sci.* 112:4773–4783.

Trowbridge, I.S., J.F. Collawn, and C.R. Hopkins. 1993. Signal-dependent membrane protein trafficking in the endocytic pathway. *Annu. Rev. Cell Biol.* 9:129–161.

Ullrich, O., S. Reinsch, S. Urbe, M. Zerial, and R.G. Parton. 1996. Rab11 regulates recycling through the pericentriolar recycling endosome. *J. Cell Biol.* 135:913–924.

Waite, R.L., J.W. Sentry, H. Stenmark, and B.H. Toh. 1998. Autoantibodies to a novel early endosome antigen 1. *Clin. Immunol. Immunopathol.* 86:81–87.

Yamashiro, D.J., B. Tycko, S.R. Fluss, and F.R. Maxfield. 1984. Segregation of transferrin to a mildly acidic (pH 6.5) para-Golgi compartment in the recycling pathway. *Cell.* 37:789–800.

Downloaded from http://rupress.org/jcb/article-pdf/156/5/797/1302370/jcb1565797.pdf by guest on 25 September 2022